JOURNAL OF MATERIALS SCIENCE 30 (1995) 2091–2096

The interpretation and use of fracture-surface morphology – a special case for polystyrene

E. K. C. LEE, A. RUDIN, A. PLUMTREE
Institute for Polymer Research, Departments of Chemical Engineering, Chemistry and Mechanical Engineering, University of Waterloo, Waterloo, Ontario N2L 3G1, Canada

The surface morphology of a system of polystyrene incorporating multilayer impact-modifier particles revealed crescent-shaped traces that could be explained as the intersection of the propagating crack and the craze zones initiated by the impact-modifier particles. This view is supported by a computer simulation which showed the variation of the shape of the intersection loci with the craze velocity/crack velocity ratio. Hence, by shape comparison or direct dimensional measurement of the crack–craze intersection, the craze velocity/crack velocity ratio at any point of the fracture surface can be determined. Together with data obtained from an instrumented Charpy impact apparatus, the craze velocity and crack velocity can be calculated. These results revealed a 100-fold increase in the crack velocity over a very short distance ($\sim 20\ \mu m$) during ductile–brittle transition. This method of interpreting and using fracture-surface morphology could be a very useful tool in studying the impact-modification phenomenon of the current system or other systems showing similar fracture-surface morphology.

1. Introduction

The interaction of crack fronts in glassy polymers, such as poly methyl methacrylate (PMMA), often result in interesting fracture-surface morphologies [1, 2]. However, such surface morphologies are often difficult to interpret and are seldom used in a quantitative manner. For glassy polymers such as PMMA and other materials, hyperbolic markings have been observed and interpreted as the intersection of primary and secondary fracture fronts during brittle fracture [3–6].

We are currently investigating the impact modification of polystyrene by emulsion-polymerized three-layer polystyrene–poly(*n*-butyl acrylate)–polystyrene particles. In the blends of polystyrene with these impact-modifier particles, unusual "crescent"-shaped traces are found around the impact-modifier particles in the ductile failure region. With the help of a computer simulation, these traces could be interpreted as the loci of intersection of the crack fronts and the craze zones around the impact-modifier particles. Hence, these traces are analogous to the hyperbolic markings of fracture fronts seen on the brittle fracture surfaces of glassy polymers mentioned above, with the difference that the current markings are the intersections of a crack front and craze zones occurring in the ductile failure region. This interpretation allows the use of the surface morphology in a quantitative way. Examples of using the fracture-surface morphology information and instrumented impact tester information to calculate crack and craze velocities in the ductile and brittle regions are demonstrated in this paper. Insight into the rapid velocity increase during ductile–brittle transitions is also obtained from the fracture-surface morphology.

2. Experimental procedure

A 33% phase volume blend of multilayer polystyrene–poly(*n*-butyl-acrylate)–polystyrene impact-modifier particles in polystyrene was made by blending the particles with a co-rotating, intermeshing twin-screw extruder. The resulting blend was then compression moulded into standard test bars for Charpy impact testing, notched and then impacted under standard testing conditions. The fracture surface was then examined using standard scanning electron microscopy, under both low and high magnifications.

3. Results and discussion

3.1. Low-magnification fracture-surface morphology

The morphology of the fracture surface under low magnification (Fig. 1) showed a relatively smooth region, which extended for about 2 mm from the notch and then changed abruptly to a region of a high degree of roughness. The extent of the smooth region corresponded to the region of a whitened surface normally associated with ductile failure and the features of the rough surface are generally associated with brittle fracture.

Fig. 1 essentially covered the ductile failure region, the ductile–brittle transition and part of the brittle failure area on the fracture surface of the test bar.

0022–2461

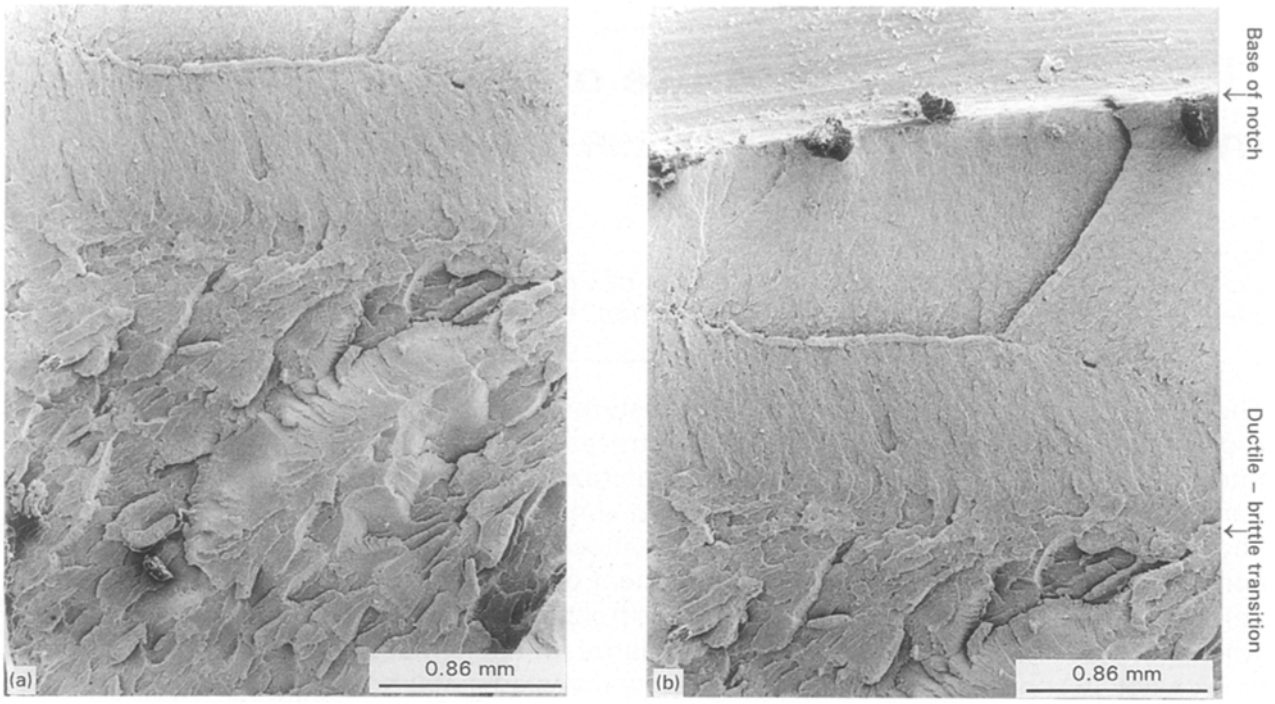

Figure 1 (a, b) Morphology of the fracture surface under low magnification.

3.2. High-magnification fracture-surface morphology

The fracture surface area corresponding to ductile failure was observed under high magnification, and a characteristic feature of crescent-shaped traces around the impact-modifier particles was observed. This extended from the base of the test-bar notch all the way to the location of the ductile–brittle transition, when these crescent-shaped traces abruptly disappeared. This sharp change was consistently observed to occur within a short distance of about 20 μm, as illustrated by Fig. 2, which is a high magnification of the ductile–brittle transition area. In this scanning electron micrograph, the failure crack propagated in the top to bottom direction. A salient feature of the crescent-shaped traces was that they were always aligned with the bow pointing towards the propagating crack, and they were always found around an impact-modifier particle.

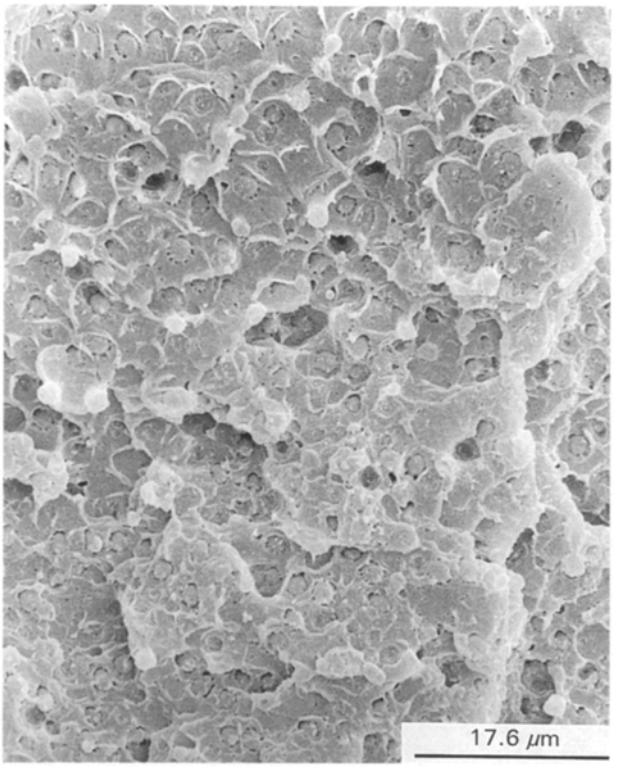

Figure 2 Morphology of ductile–brittle transition region under high magnification.

3.3. Crescent shapes as intersection loci of crack and crazes

It is generally accepted that polystyrene undergoes crazing exclusively when stressed under tension. In the case of polystyrene modified with impact-modifier particles, these crazes are generally initiated at the equator of rubber particles, which are the locations of maximum principal stresses, and propagate radially outward [7]. In fact, the function of impact-modifier particles in polystyrene is generally accepted to relate to their ability to generate profuse crazing which absorbs the energy of impact. At the same time, the rubbery particles act as craze terminators and load-bearing elements in the stabilization of the crazes.

With this view of the role of the impact-modifier particles as sites for craze initiation and growth, the crescent-shaped crazes could be explained as the loci of intersection between a propagating crack front and the radiating crazes from the impact-modifier particles. This approach is similar to that used to explain the formation of hyperbolic markings on brittle fracture surfaces as the intersections of fracture fronts [3, 4]. Fig. 3 illustrates schematically the intersection of a propagating crack front (represented by parallel lines) and a radiating craze front travelling at the same

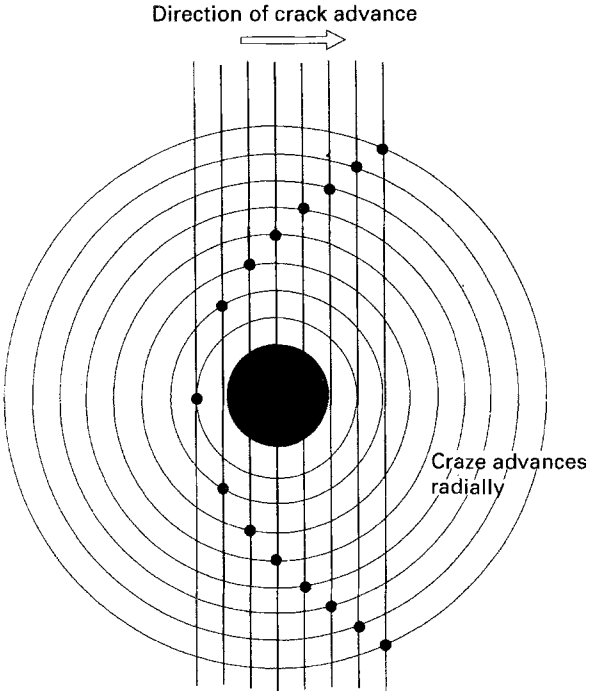

Figure 3 Schematic drawing of crack–craze intersection.

speed (represented by concentric circles) from an impact-modifier particle. It can be seen that the points of intersection in time sequence form a parabolic crescent shape, aligned with the bow of the crescent pointing towards the propagating crack.

A computer program was written to simulate the intersection of a propagating parallel crack front with a radiating circular craze front (see Appendix). The results for various craze velocity/crack velocity ratios are given in Fig. 4a–d. In this figure, the circle represents the craze front at the instant when the crack front first meets the craze front, and the other curve represents the loci of intersection between the advancing crack and the radiating craze. It can be seen that, on progressive increase of the crack velocity, the intersection curve changes from a parabolic crescent to an ellipse and finally to a near circle closely surrounding the initial craze front.

3.4. Measurement of the ratio of crack velocity to craze velocity

The variation of the shape of the crack–craze intersection loci with the craze velocity/crack velocity ratio points to a method of estimating the ratio of those velocities under the actual fracture conditions. A simplistic approach would be simply to compare the shapes of the crescents found on the fracture surface to a series of shapes generated by the computer simulation, and finding the closest match. Another method would be through the direct measurement of the dimensions of the crescents. Such a procedure is illustrated with an idealized intersection curve in Fig. 5. The craze velocity/crack velocity ratio is given by the ratio of distances a to d in the figure. This is because it takes the same amount of time for the craze front to travel the distance a as it takes the crack front to travel distance d.

A set of direct-measurement data of the clearly defined crescents on the ductile failure region in Fig. 2, performed on a magnified photograph, is given in Table I. The material in this sample contains 33% by volume of three-layer polystyrene–poly(*n*-butyl acrylate)–polystyrene particles of 2.5 μm diameter. The polystyrene matrix is Styron® 685D (Dow Chemical Company), a general purpose grade of ~300 000 weight average molecular weight. The value of the craze velocity/crack velocity ratio was measured to be 0.70, with a standard deviation of 0.055.

3.5. Measurement of crack and craze velocities in the ductile region

Having measured the craze velocity/crack velocity ratio in the ductile failure region, we can calculate the craze velocity if the crack velocity is known. Because the Charpy impact was conducted on an instrumented apparatus [8], the force–time trace for the impact event was available, which is shown in Fig. 6. The ductile failure phase of the impact event is recorded in the rising part of the force–time trace, and ends at the point of maximum load. The duration of the brittle failure phase of the impact event is measured as the time for the load to drop to zero from the maximum. The length of the ductile failure region can be measured from the low-magnification scanning electron micrograph in Fig. 1. Knowing the duration of the ductile failure phase and the length of the ductile region, the crack velocity during the ductile failure phase can be calculated. The craze velocity in the ductile region can then be calculated from the crack velocity using the craze velocity/crack velocity ratio previously measured.

From Figs 6 and 1, the duration of the ductile failure phase was 790 μs and the length of the ductile region was 2 mm. Hence the crack velocity in the ductile failure phase was $\sim 2.5\ m\,s^{-1}$ and the craze velocity was $0.7 \times 2.5\ m\,s^{-1} = 1.8\ m\,s^{-1}$.

3.6. Crack velocity in the brittle failure region

The crack velocity in the brittle failure region can be estimated from the shape of the crack–craze intersection curve in the brittle failure region. From Fig. 2, it can be seen that the crack–craze intersection undergoes a sudden change from crescent-shaped to circular-shaped across the ductile–brittle transition. According to the computer simulation of the shape of the crack–craze intersection, this corresponds to a sudden increase of the crack velocity by a 100 fold, because the shape of the intersection changed from that of Fig. 4a (craze velocity/crack velocity ratio = 0.7) to Fig. 4d (ratio = 0.007). Hence, from the shape of the crack–craze intersection, the crack velocity in the brittle is $2.5\ m\,s^{-1} \times 100 = 250\ m\,s^{-1}$.

This value of the crack velocity in the brittle region is supported by independent calculation of the brittle failure phase and the length of the brittle failure

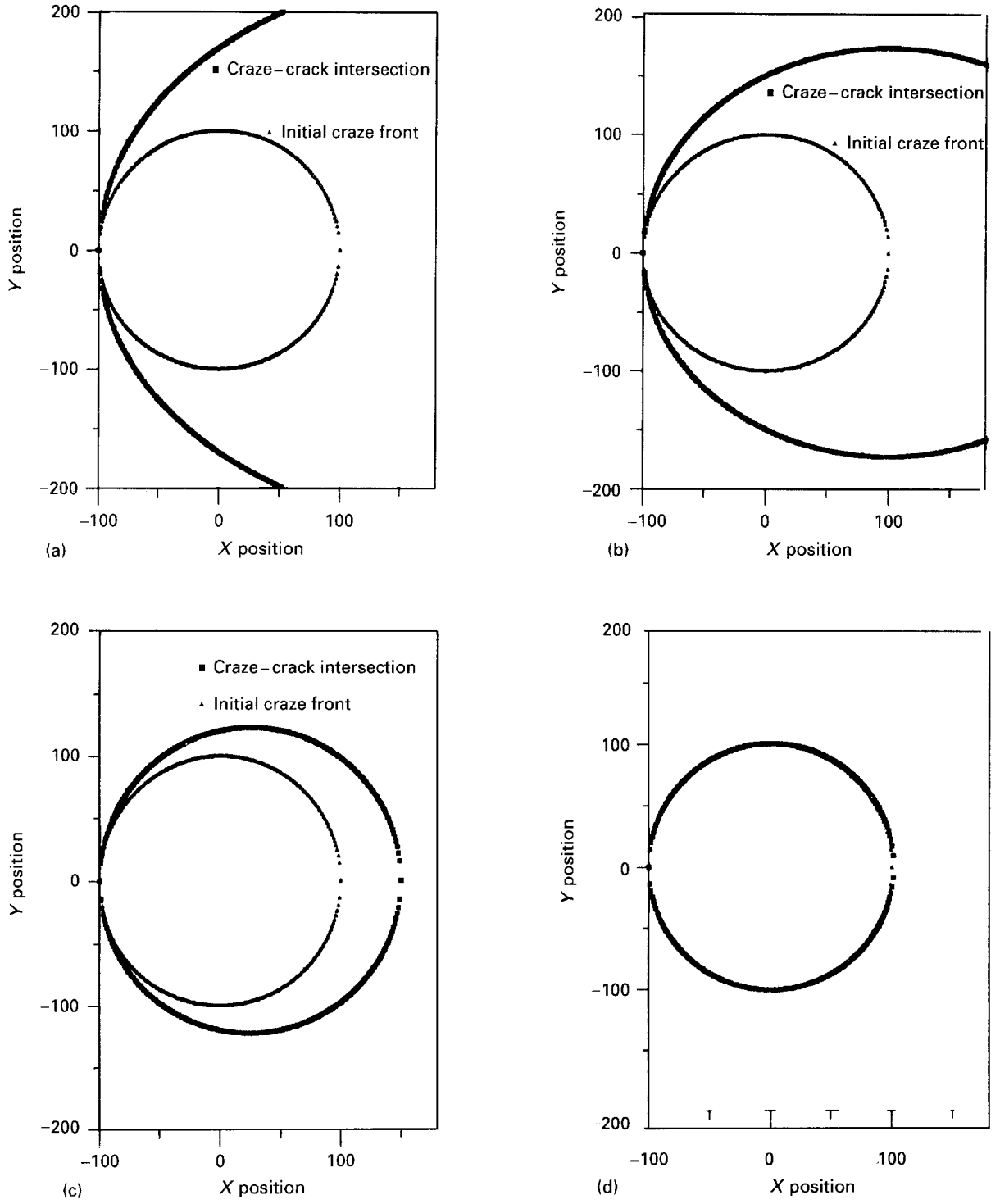

Figure 4 Computer simulation of crack–craze intersection. Craze velocity/crack velocity: (a) 0.7, (b) 0.5, (c) 0.2, (d) 0.007.

region. From Fig. 6, the duration of the brittle failure during the Charpy impact event is 30 μs. The test-bar width is 12.5 mm, given a notch depth of 2.5 mm and a ductile region length of 2 mm, the remaining brittle region is 8 mm long. This gives a brittle crack velocity of 8 mm/30 μs = 267 m s^{-1}, which corresponds very closely to the 250 m s^{-1} by estimation from the shape of the crack–craze intersection.

The interesting fact is that the crack velocity undergoes such a dramatic increase within such a short distance (~ 20 μm) during the ductile–brittle transition. There have been observations on the sudden increase of crack velocity at ductile–brittle transition, e.g. PMMA [9]. However, no prior work seems to exist that allows the estimation of this crack-velocity jump directly from the morphology of the fracture surface of the test specimen.

4. Conclusions

1. The crescents on the fracture surface are the loci of intersection of the propagating crack with crazes radiating from impact-modifier particles.
2. By using a computer simulation, the shape of the crack–craze intersection curve is shown to be a function of the craze velocity/crack velocity ratio.
3. From the fracture surface morphology, by either shape comparison with computer simulated curves or

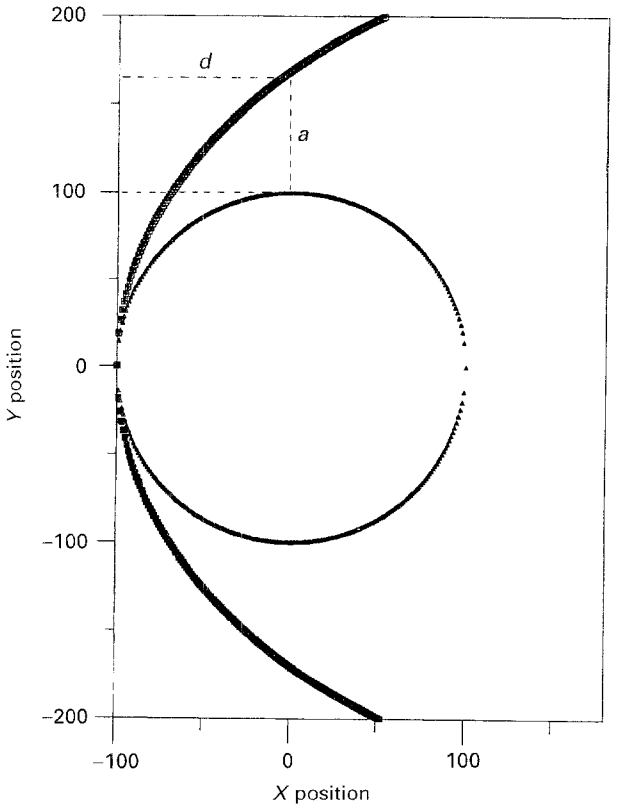

Figure 5 Craze velocity/crack velocity ratio by direct measurement (= a/d).

TABLE I Craze velocity/crack velocity ratio in the ductile region from direct measurement of crescent dimensions on magnified photograph

Crescent	2(a + d) in mm	d in mm	a/d (= craze/crack velocity ratio)
1	13.0	4.0	0.63
2	12.5	3.5	0.78
3	9.0	2.6	0.73
4	10.5	3.2	0.64
5	11.5	3.5	0.64
6	11.5	3.3	0.74
7	10.5	3.0	0.75
8	11.0	3.2	0.72
9	11.5	3.5	0.64
10	8.5	2.5	0.70
			Average = 0.70
			s = 0.055

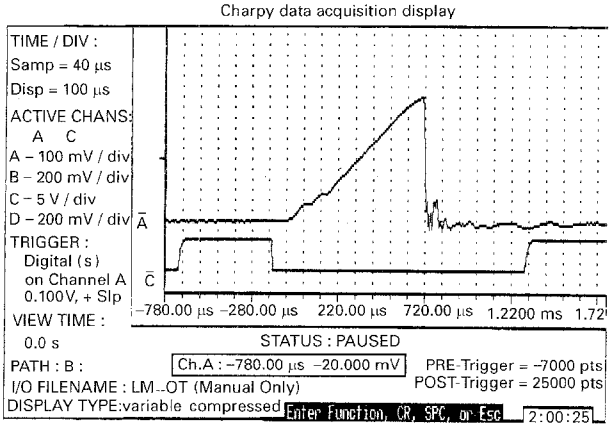

Figure 6 Force–time trace from instrumented Charpy impact.

direct dimensional measurement, the craze velocity/crack velocity ratio at any point of the fracture surface can be determined.

4. The crack velocity in the ductile and brittle regions can be calculated using time data from the force–time trace of the instrumented Charpy impact tester and the length of the ductile region from the fracture surface.

5. The craze velocity can be calculated using the ductile region crack velocity and the craze/crack velocity ratio determined in 3.

6. The crack velocity was estimated to increase 100-fold across a very short distance (~ 20 µm) at the point of ductile–brittle transition. This velocity change was confirmed by independent calculation of crack velocity in the brittle region from instrumented impact force–time data and specimen dimensional measurement.

7. Starting from the morphology of the fracture surface, the above methodology allows the calculation of craze and crack velocities in both the ductile and brittle region of failure for the current system of polystyrene/impact modifier system being studied. These are important parameters in the impact performance of the system. It may be possible to use this method on systems showing a similar fracture-surface morphology.

Acknowledgements

The authors thank The Dow Chemical Company, the Ontario Centre for Materials Research, and the Natural Science and Engineering Research Council, for their financial support. The stimulating discussions with Dr Morris Rogers and Dr Mark Soderquist of Dow Chemical are greatly appreciated.

Appendix: listing of the computer program for the simulation of crack–craze intersection

```
CLS
100     INPUT ''Radius of craze at
        initial contact:'', r
110     INPUT ''Ratio of craze velocity
        to crack velocity:'', k
120     INPUT ''FileName to Use?'', q$
130     OPEN ''B:\'' + q$ FOR OUTPUT AS
        #1
140     interval = r/100
150     FOR a = 0 TO 3 * r STEP interval
160     x = - r + a
162     IF (r + k * a) ^ 2 > = x ^ 2 THEN
170       Y = SQR ((r + k * a) ^ 2 - x ^ 2)
172     ELSE GOTO 260
174     END IF
180     IF a <= 2 * r THEN
190       Z = SQR (r ^ 2 - x ^ 2)
200       PRINT #1, x, CHR$ (9), Y, CHR$
        (9), - Y, CHR$ (9), Z, CHR$ (9), - Z
210       PRINT x, Y, - Y, Z, - Z
220     ELSE PRINT #1, x, CHR$ (9), Y,
          CHR$ (9), - Y
```

```
230         PRINT x, Y, -Y
240       END IF
250       NEXT a
260       CLOSE #1
270       END
```

References

1. W. DÖLL, *J. Mater. Sci.* **10** (1975) 935.
2. R. P. KUSY and D. T. TURNER, *Polymer* **18** (1977) 391.
3. W. DÖLL, in "Fractography and Failure Mechanisms of Polymers and Composites", edited by Anne C. Roulin-Moloney (Elsevier Applied Science, London, 1989) p. 398.
4. J. WOLOCK and S.B. NEWMAN, in "Fracture Processes in Polymeric Solids", edited by B. Rosen (Interscience, New York, 1964) p. 235.
5. J. A. KIES, A. M. SULLIVAN and G. R. IRWIN, *J. Appl. Phys.* **21** (1950) 716.
6. J. LEEUWERIK, *Rheol. Acta* **2** (1962) 10.
7. C. B. BUCKNALL, "Toughened Plastics" (Applied Science, London, 1977) p. 189.
8. D. COOK, PhD thesis, University of Waterloo (1992).
9. W. DÖLL, in "Polymer Fracture", 2nd edn, edited by H. H. Kausch (Springer, Berlin, 1987) pp. 313, 383.

Received 17 January
and accepted 11 August 1994